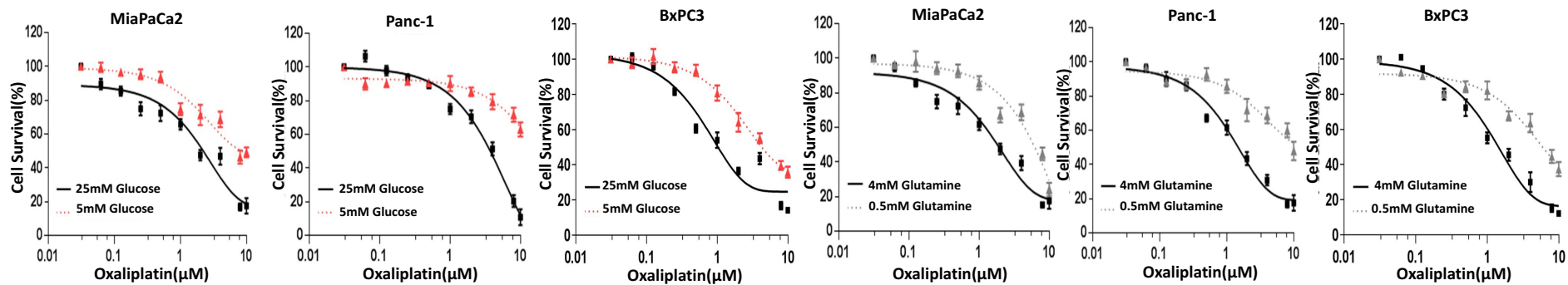
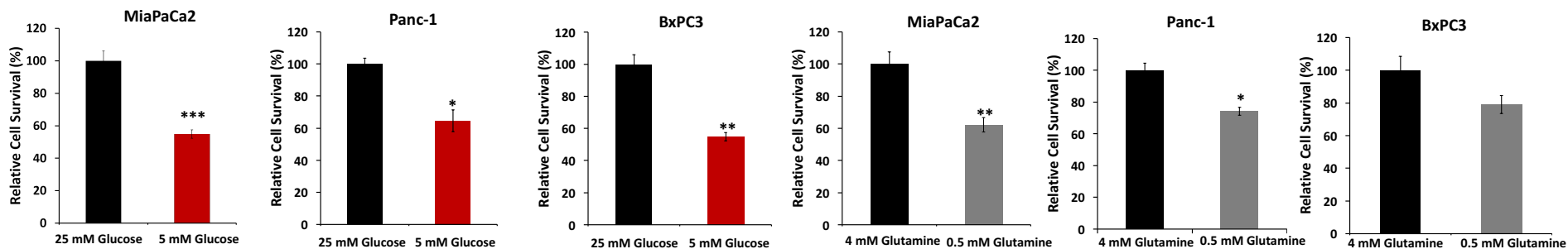
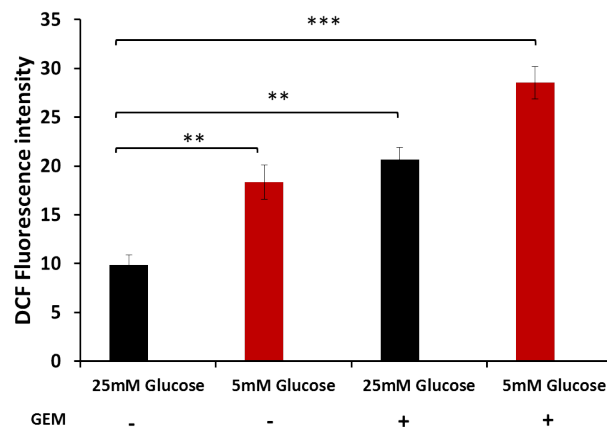


AOxaliplatin IC50 Values (\pm SEM), μ M

| | 25 mM Glucose | 5mM Glucose | Fold Difference 5 mM VS 25mM | p-value(two-tailed) | 4mM Glutamine | 0.5mM Glutamine | Fold Difference 0.5 mM VS 4mM | p-value(two-tailed) |
|----------|---------------|-------------|---------------------------------|---------------------|---------------|-----------------|----------------------------------|---------------------|
| MiaPaCa2 | 1.82 (0.041) | 8.22 (0.53) | 4.51 | < 0.0047 | 1.63 (0.034) | 5.41 (0.037) | 5.61 | < 0.001 |
| Panc-1 | 3.25 (0.027) | >10 | >10 | NA | 1.52 (0.033) | >10 | >10 | < 0.0032 |
| BxPC3 | 1.37 (0.064) | 6.98 (0.06) | 5.09 | < 0.0026 | 1.44 (0.068) | 8.653 (0.012) | 6.09 | < 0.001 |

B**C****Figure S1**

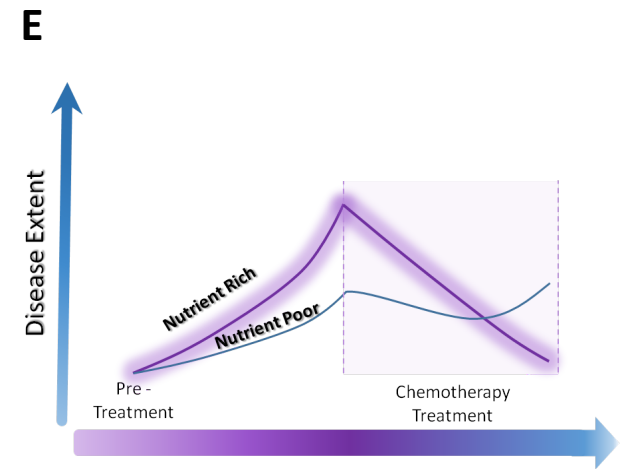
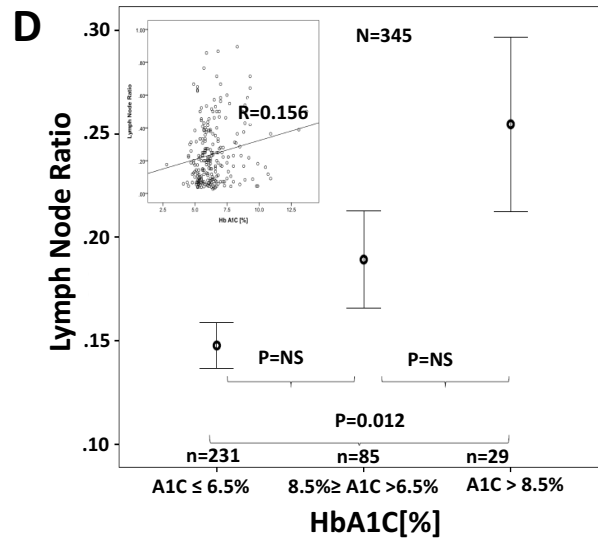
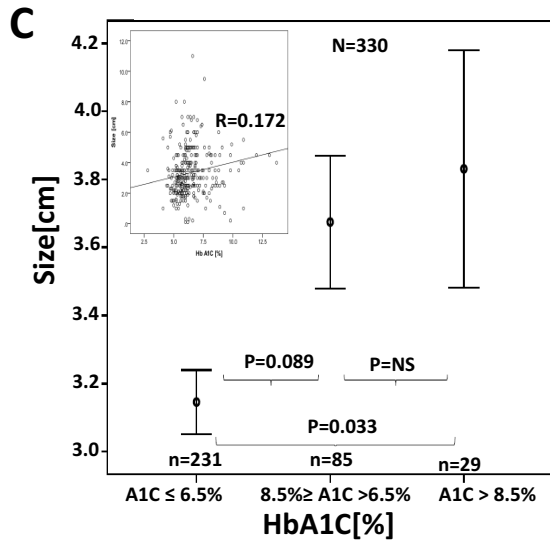
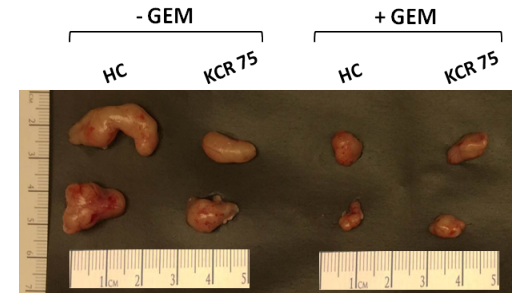
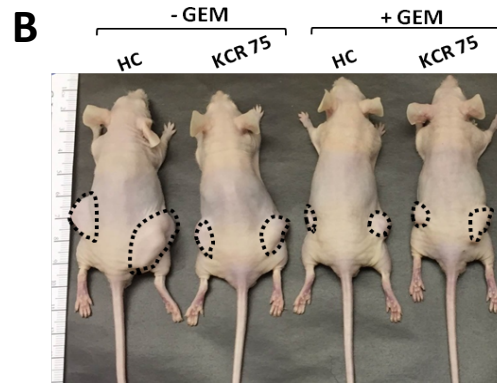
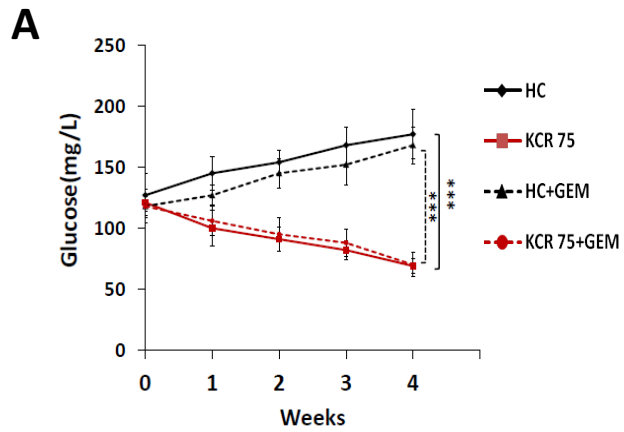
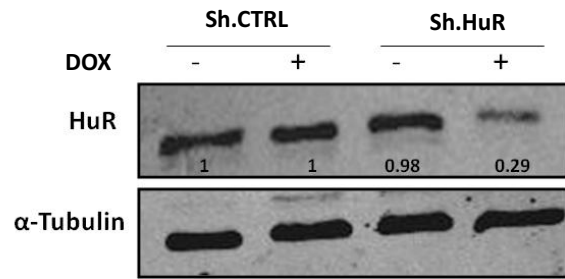
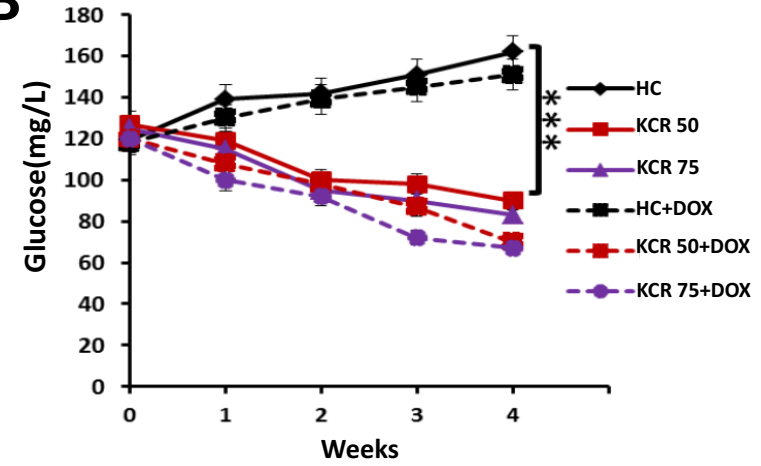
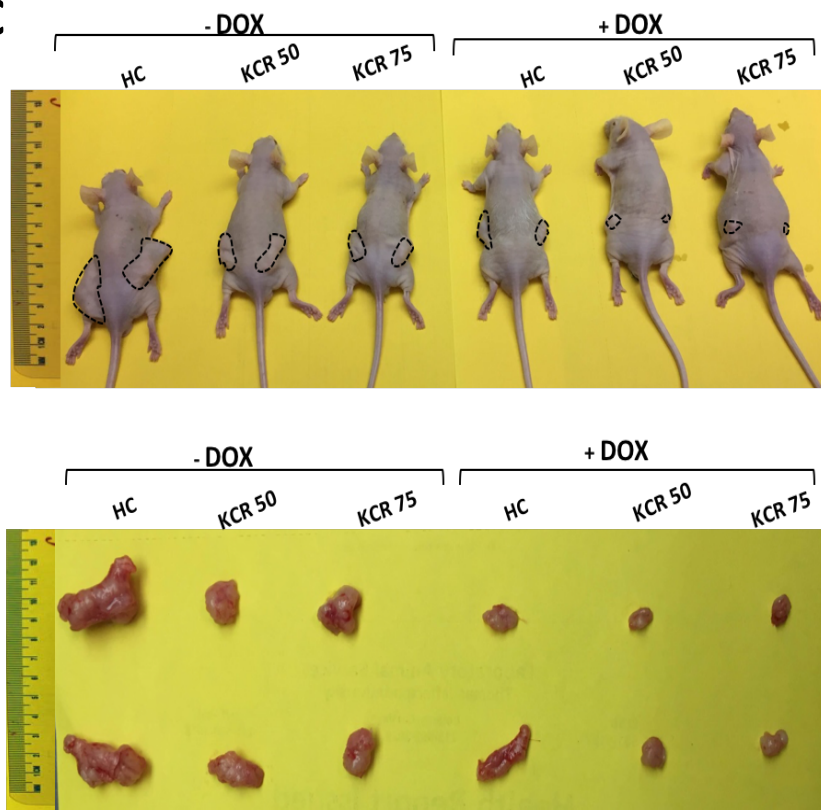
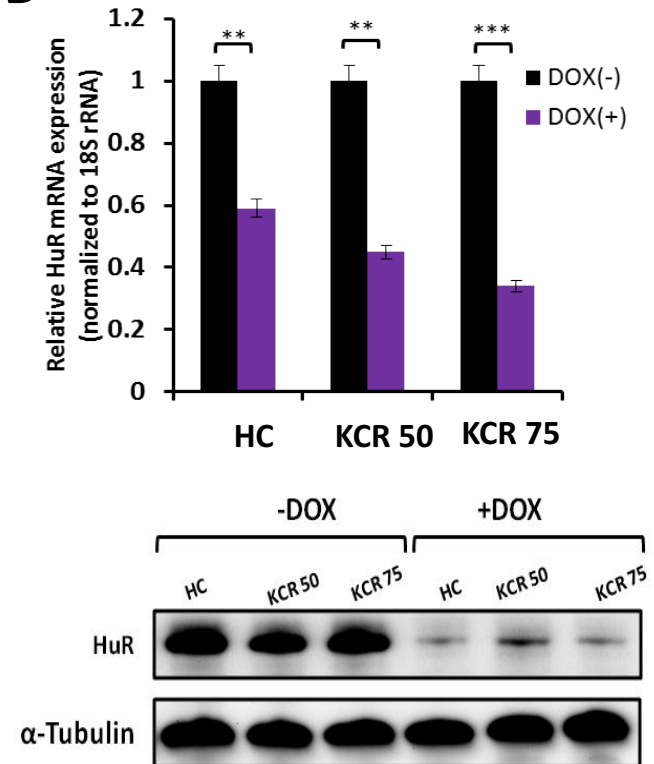
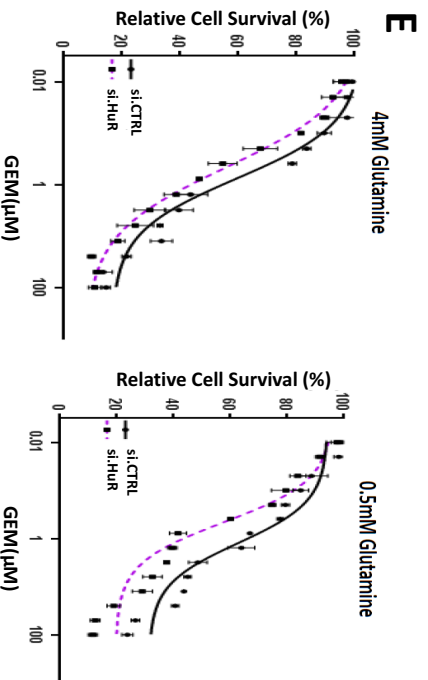
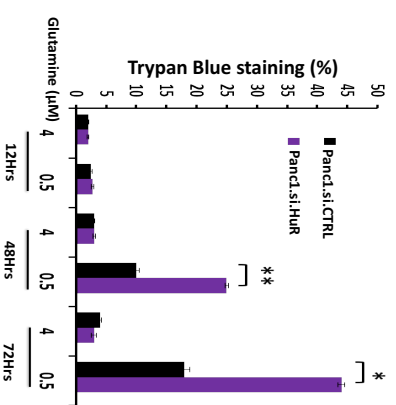
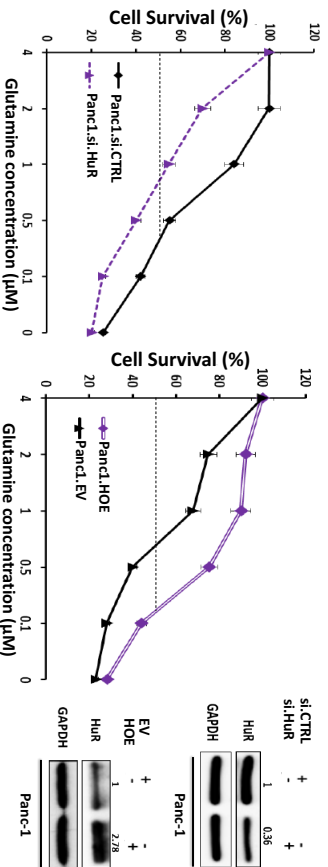
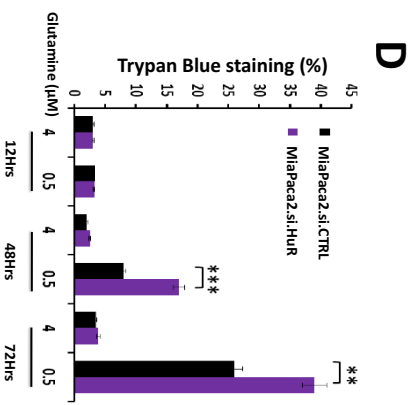
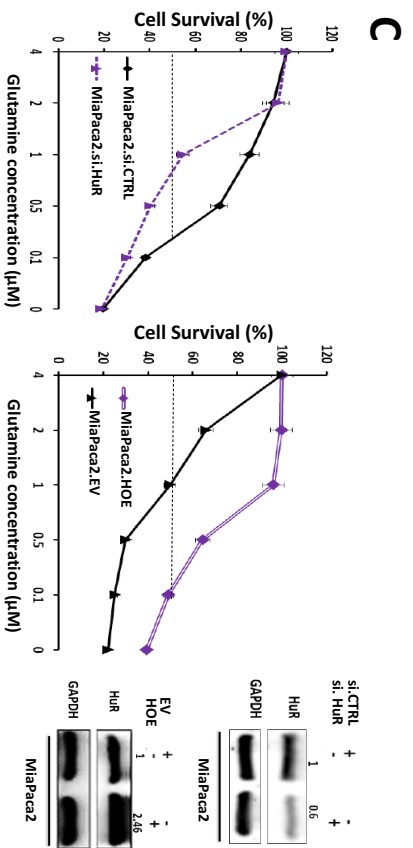
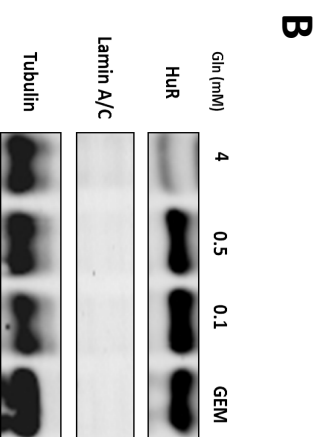
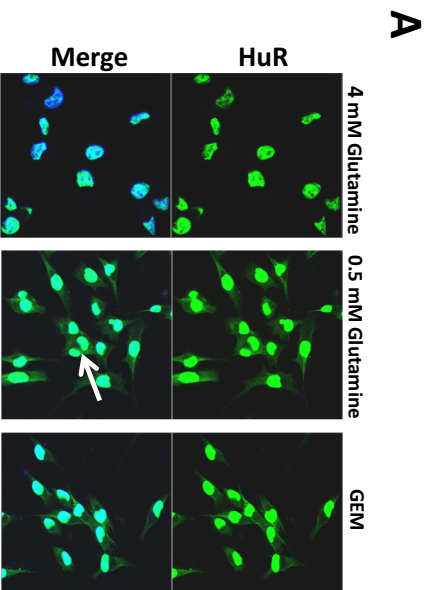


Figure S2

A**B****C****D****Figure S3**



| GEM IC50 Values (\pm SEM) μM | | Fold Difference | | p-value (two-tailed) | |
|--|-------------|-----------------|-------|----------------------|----------|
| siCTRL | siHuR | siCTRL | siHuR | siCTRL vs siHuR | |
| 4mM Glutamine | 0.70 (0.14) | 0.41 | 0.28 | 1.70 | < 0.0043 |
| 0.5mM Glutamine | 2.94 (0.38) | 0.56 | 0.19 | 5.06 | < 0.0008 |

Figure S4

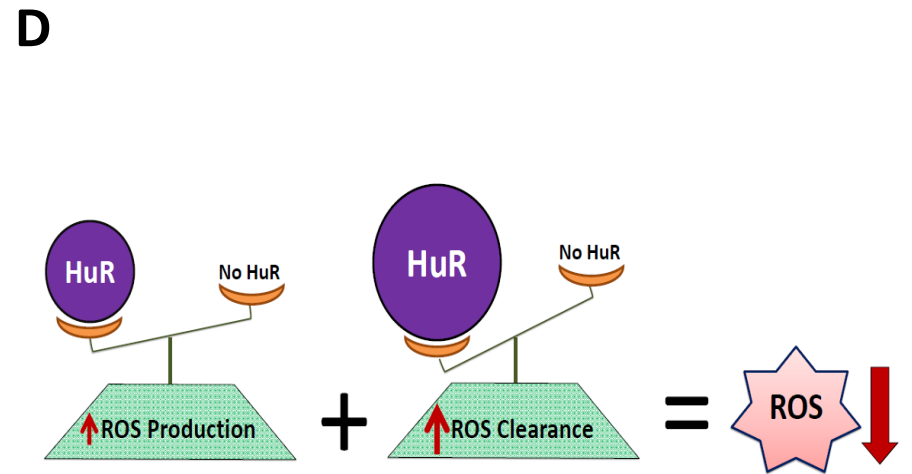
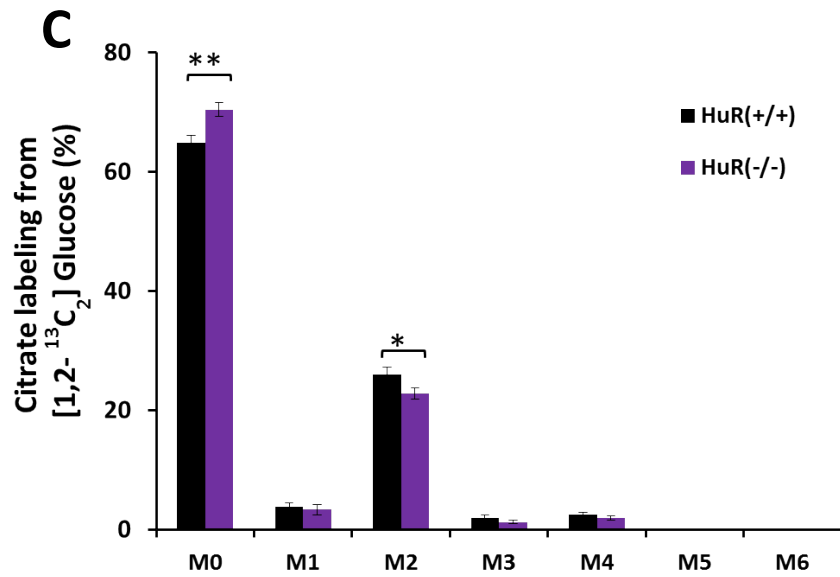
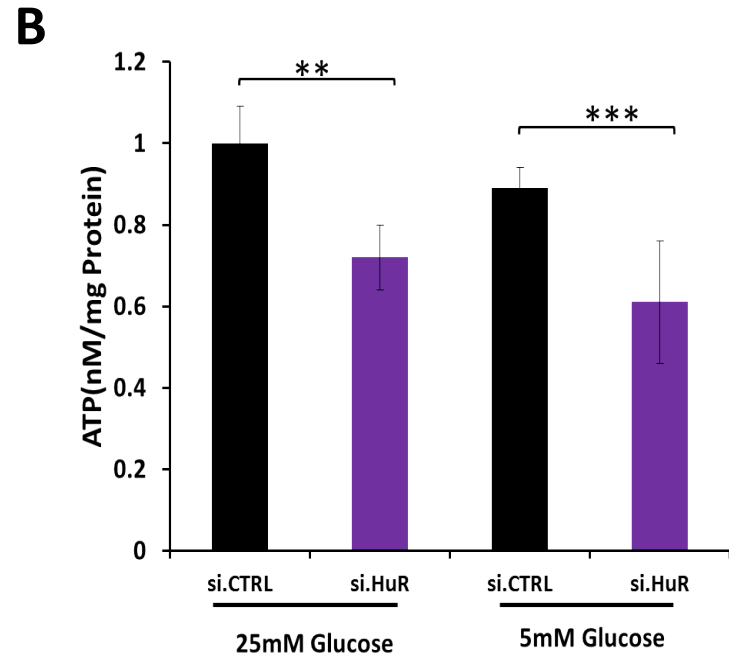
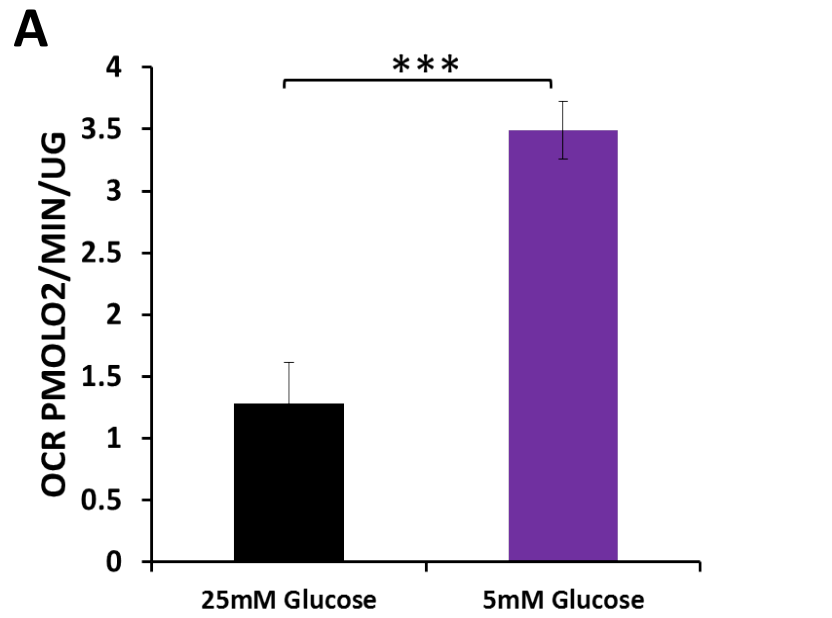


Figure S5

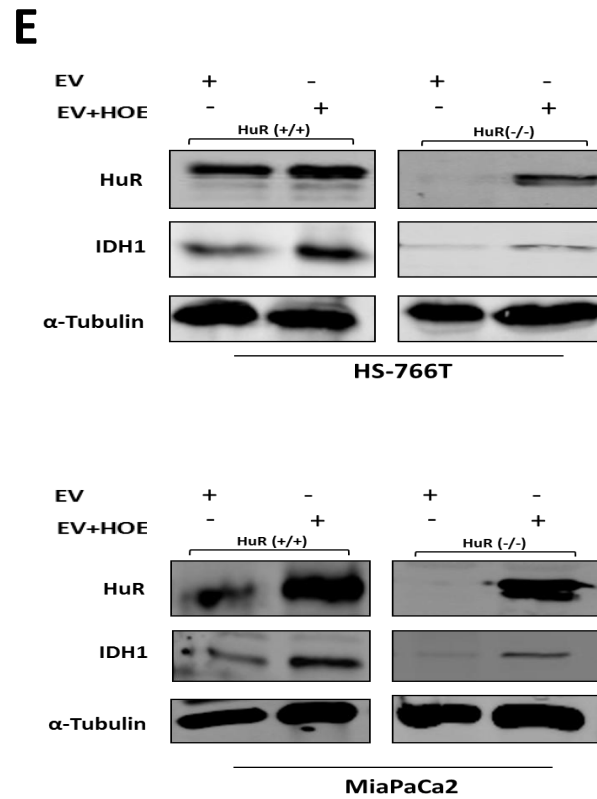
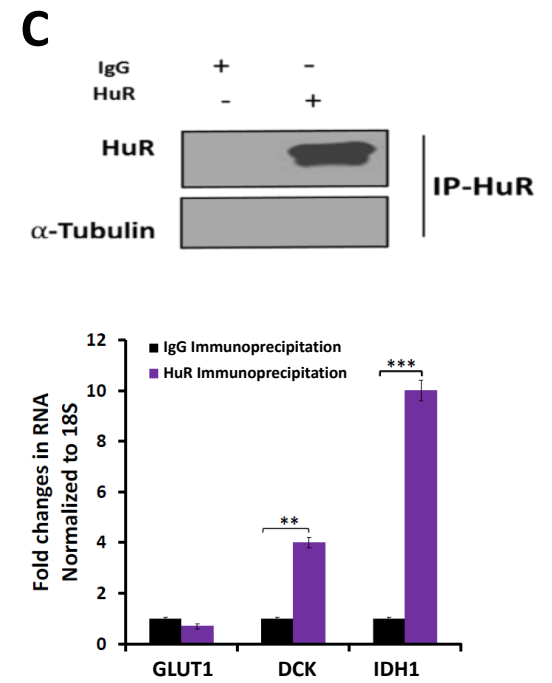
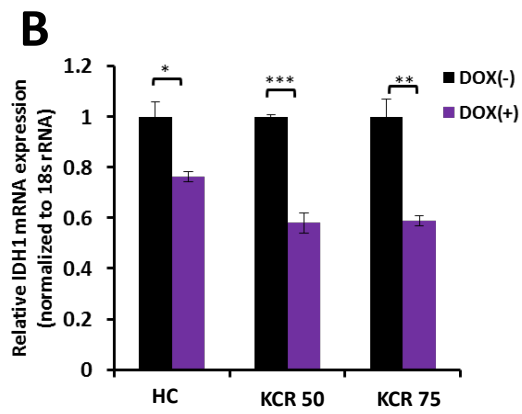
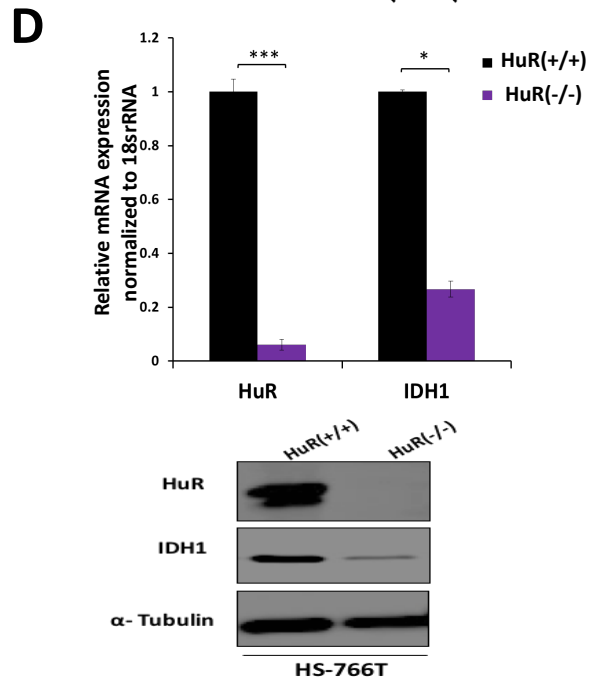
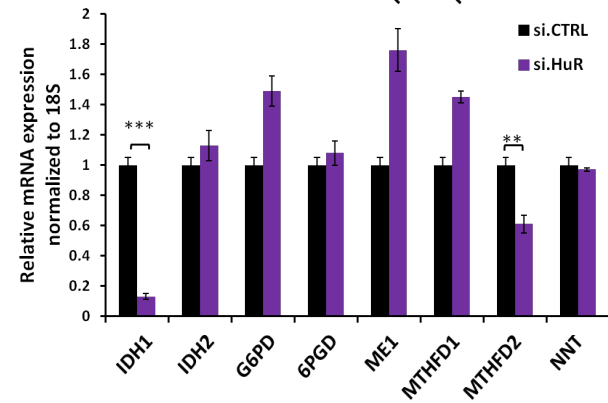
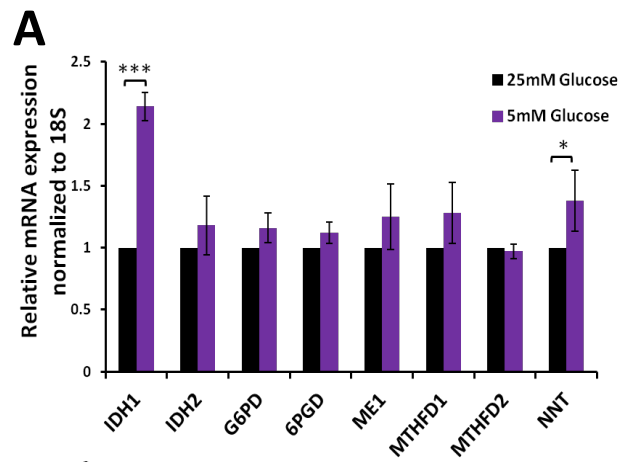


Figure S6

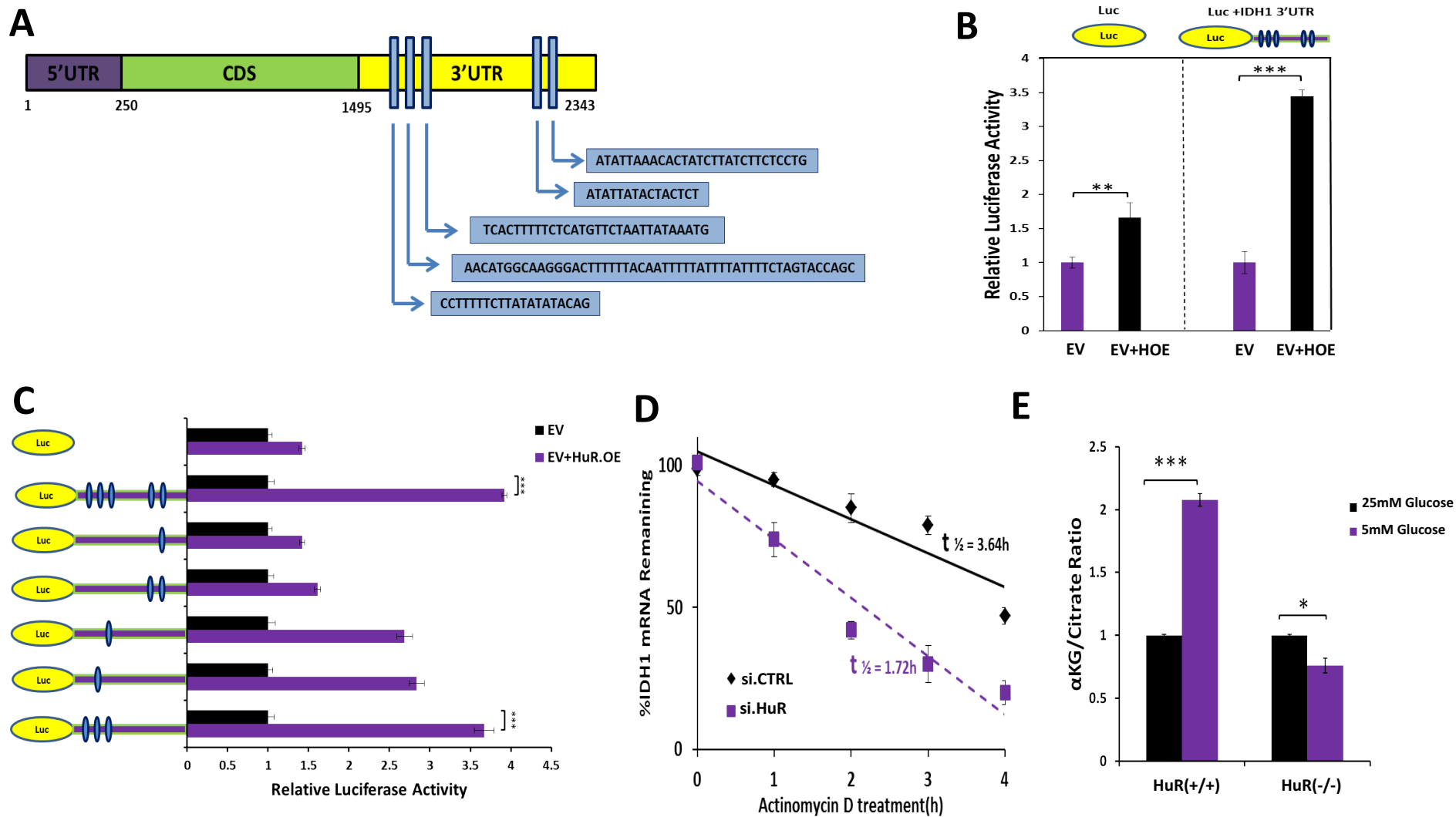


Figure S7

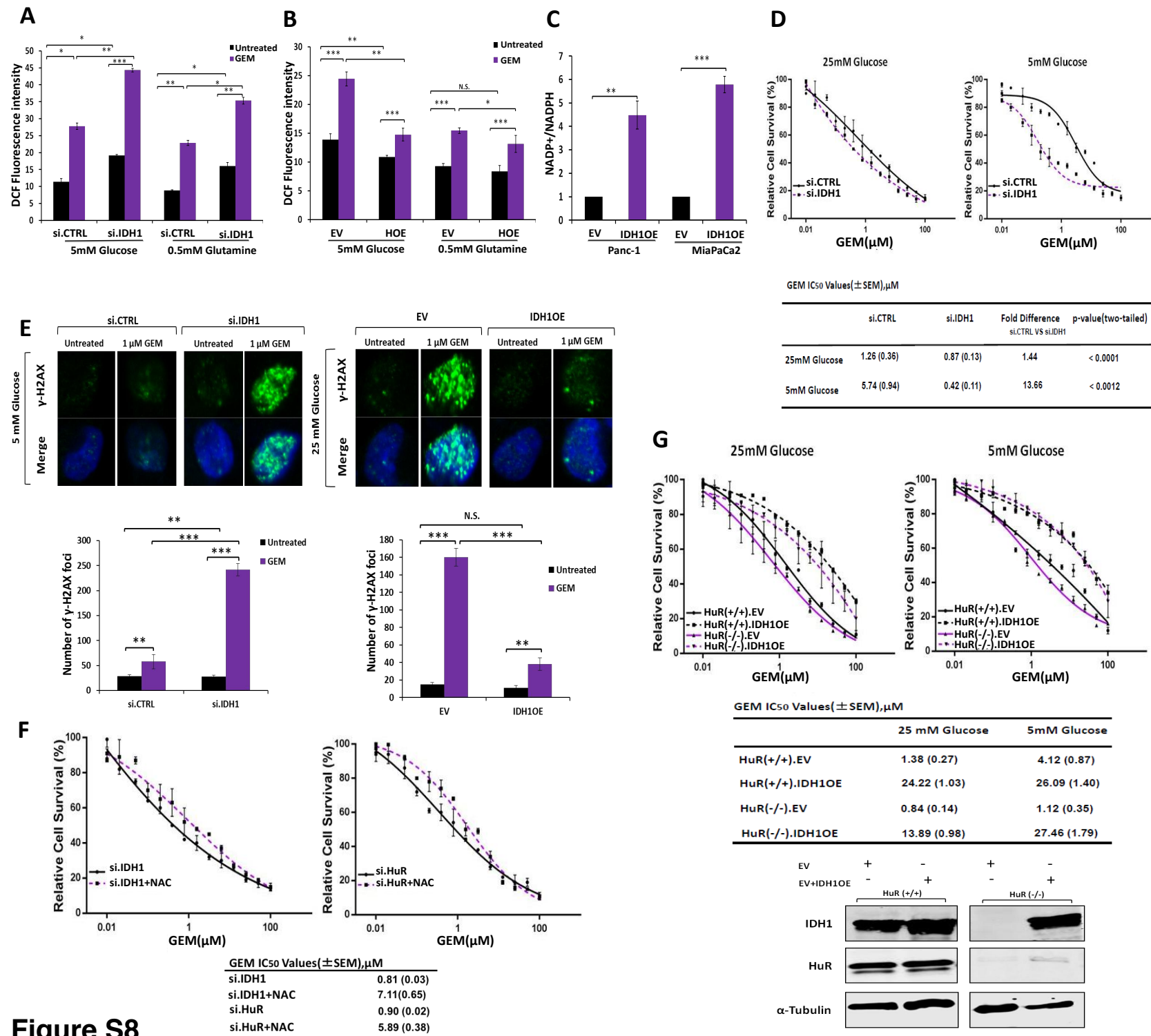


Figure S8

Supplemental Tables

Table S1: Nomenclature used throughout manuscript to describe genetically modified cell lines.

| Name | Transfection procedure |
|---------------------|---|
| MiaPaCa2.si.CTRL | siRNA transfection of scrambled control |
| MiaPaCa2.si.HuR | siRNA transfection against HuR |
| MiaPaCa2.si.IDH1 | siRNA transfection against IDH1 |
| Panc-1.si.CTRL | siRNA transfection of scrambled control |
| Panc-1.si.HuR | siRNA transfection against HuR |
| MiaPaCa2.EV | Plasmid transfection of empty vector |
| MiaPaCa2.HOE | Plasmid transfection of HuR |
| Panc-1.EV | Plasmid transfection of empty vector |
| Panc-1.HOE | Plasmid transfection of HuR |
| MiaPaCa2.IDH1OE | Plasmid transfection of IDH1 |
| MiaPaCa2.sh.CTRL | shRNA stable transfection of scrambled control |
| MiaPaCa2.sh.HuR | shRNA stable transfection against HuR [doxycycline inducible suppression of HuR] |
| Mia.HuR(-/-) | CRISPR/Cas9-mediated knockout of HuR using a guide RNA targeting HuR in MiaPaca2 cells |
| Mia.HuR(+/+) | CRISPR/Cas9- scrambled control in MiaPaca2cells |
| HS.HuR(-/-) | CRISPR/Cas9-mediated knockout of HuR using a guide RNA targeting HuR in HS-766T cells |
| HS.HuR(+/+) | CRISPR/Cas9- scrambled control in HS-766T cells |
| Mia.HuR(-/-).EV | Stable overexpression of empty vector in CRISPR/Cas9 mediated knockout of HuR in MiaPaca2 cells |
| Mia.HuR(-/-).IDH1OE | Stable overexpression of IDH1 in CRISPR/Cas9 mediated knockout of HuR in MiaPaca2 cells |

Table S2. Patient Cohort Characteristics

| | Total (N= 107) | HG (n=86) | NG (n=21) | P |
|----------------------------------|-----------------------|------------------|------------------|-----------|
| | N(%) | N(%) | N(%) | |
| Gender | | | | |
| Male | 56 (52%) | 45 (52%) | 11 (52%) | <i>NS</i> |
| Female | 51 (48%) | 41 (48%) | 10 (48%) | |
| Race | | | | |
| White/European | 95 (89%) | 76 (89%) | 19 (90%) | |
| African American | 9 (8%) | 8 (9%) | 1 (5%) | <i>NS</i> |
| Asian | 2 (2%) | 1 (1%) | 1 (5%) | |
| Other | 1 (1%) | 1 (1%) | 0 (0%) | |
| BMI | 28.0 (±6.1) | 28.3 (±6.3) | 26.9 (±4.7) | <i>NS</i> |
| Age | 65.9 (±10.4) | 65.9(±10.0) | 65.9 (±12.3) | <i>NS</i> |
| Procedure | | | | |
| Classic Whipple | 17 (16%) | 13 (15%) | 4 (19%) | |
| PPPD | 64 (60%) | 49 (57%) | 15 (71%) | <i>NS</i> |
| Distal Pancreatectomy | 23 (21%) | 22 (26%) | 1 (5%) | |
| Total Pancreatectomy | 3 (3%) | 2 (2%) | 1 (5%) | |
| Histopathology | | | | |
| Tumor Size | 3.5 (±1.5) | 3.7 (±1.5) | 3.0 (±1.2) | § |
| High Tumor Grade | 20 (19%) | 14 (16%) | 6 (29%) | <i>NS</i> |
| Metastatic Lymph Nodes | 75 (70%) | 60 (70%) | 15 (71%) | <i>NS</i> |
| LNR | 0.16 (±0.18) | 0.15 (±0.17) | 0.19 (±0.21) | <i>NS</i> |
| Involved Surgical Margins | 35 (33%) | 28 (32%) | 7 (33%) | <i>NS</i> |
| Perineural Invasion | 95 (89%) | 80 (93%) | 15 (71%) | * |

Categorical parameters are presented as absolute count and percentages in parenthesis. Continuous parameters are presented as means (±SD). PPPD, *Pylorus Preserving Pancreatoduodenectomy*. Lymph node ratio was calculated as number of metastatic lymph nodes/total number of lymph nodes recovered from the surgical specimen. *NS*, Non-Significant. Statistical significance of $P < 0.05$ is marked with an asterisk (*). § - Statistical trend ($P = 0.1-0.05$).

Table S4. List of Enzymes directly involved in the anti-oxidant defense response.

| Gene Name | Gene Symbol | Classification/Pathway |
|---|-------------|--|
| 6-phosphogluconate dehydrogenase | 6PGD | NADPH regeneration/Pentose Phosphate |
| Glucose-6-phosphate dehydrogenase | G6PD | NADPH regeneration/Pentose Phosphate |
| Isocitrate Dehydrogenase 1 | IDH1 | NADPH regeneration/Krebs |
| Isocitrate Dehydrogenase 2 | IDH2 | NADPH regeneration/Krebs |
| Malic Enzyme 1 | ME1 | NADPH regeneration/Krebs |
| Methylenetetrahydrofolate dehydrogenase 1 | MTHFD1 | NADPH regeneration/Folate |
| Methylenetetrahydrofolate dehydrogenase 2 | MTHFD2 | NADPH regeneration/Folate |
| Nicotinamide Nucleotide Transhydrogenase | NNT | NADPH regeneration/NAD |
| Catalase | CAT | Antioxidants/Catalases/free radical detoxification |
| Glutamate-cysteine ligase catalytic subunit | GCLC | Antioxidants/Glutathione synthesis |
| Glutamate-cysteine ligase modifier subunit | GCLM | Antioxidants/Glutathione synthesis |
| Glutathione peroxidase1 | GPx1 | Antioxidants/Glutathione Peroxidases/free radical detoxification |
| Glutathione peroxidase2 | GPx2 | Antioxidants/Glutathione Peroxidases/free radical detoxification |
| Glutathione peroxidase3 | GPx3 | Antioxidants/Glutathione Peroxidases/free radical detoxification |
| Glutathione peroxidase4 | GPx4 | Antioxidants/Glutathione Peroxidases/free radical detoxification |
| Glutathione peroxidase5 | GPx5 | Antioxidants/Glutathione Peroxidases/free radical detoxification |
| Glutathione peroxidase6 | GPx6 | Antioxidants/Glutathione Peroxidases/free radical detoxification |
| Glutathione peroxidase7 | GPx7 | Antioxidants/Glutathione Peroxidases/free radical detoxification |
| Glutathione S-transferase | GST | Antioxidants/Glutathione synthesis/free radical detoxification |
| Glutathione synthetase | GSS | Antioxidants/Glutathione synthesis/free radical detoxification |
| Superoxide dismutase 1 or Copper-zinc SOD | SOD1 | Antioxidants/Superoxide Metabolism |
| Superoxide dismutase 2 or Manganese SOD | SOD2 | Antioxidants/Superoxide Metabolism |
| Superoxide dismutase 3 or Extracellular SOD | SOD3 | Antioxidants/Superoxide Metabolism |
| Glutaredoxin1 | GRX1 | Redox |
| Glutaredoxin2 | GRX2 | Redox |
| Glutaredoxin3 | GRX3 | Redox |
| Glutaredoxin4 | GRX4 | Redox |
| Glutaredoxin5 | GRX5 | Redox |
| Glutathione Reductase | GR | Redox |
| peroxiredoxin 1 | PRDX1 | Redox |
| peroxiredoxin 2 | PRDX2 | Redox |
| peroxiredoxin 3 | PRDX3 | Redox |
| peroxiredoxin 4 | PRDX4 | Redox |
| peroxiredoxin 5 | PRDX5 | Redox |
| peroxiredoxin 6 | PRDX6 | Redox |
| Thioredoxin reductase 1 | TXNRD1 | Redox |
| Thioredoxin reductase 2 | TXNRD2 | Redox |
| Thioredoxin reductase 3 | TXNRD3 | Redox |
| Thioredoxin1 | TXN 1 | Redox |
| Thioredoxin2 | TXN 2 | Redox |

Table S5: Results of RNA sequencing in PDA cell lines (HS-766T and MiaPaCa2) with each modulated by CRISPR/Cas9 to delete HuR expression.

| Gene Symbol | HS | | | Mia | | |
|-------------|--|---------|---------|--|---------|---------|
| | Log2 Fold Change (HuR(+/+)vsHuR(-/-); <=0 is down in HuR(-/-)) | pValue | FDR | Log2 Fold Change (HuR(+/+)vsHuR(-/-); <=0 is down in HuR(-/-)) | pValue | FDR |
| IDH1 | -6.18610 | 0.00000 | 0.00000 | -4.19733 | 0.00078 | 0.00738 |
| ELAVL1 | -4.50754 | 0.00000 | 0.00000 | -2.47939 | 0.00000 | 0.00000 |
| GPx3 | 0.78045 | 0.00418 | 0.02155 | -1.25985 | 0.00001 | 0.00022 |
| GRX3 | 0.56216 | 0.00112 | 0.00720 | -0.54306 | 0.00413 | 0.02847 |
| SOD2 | 0.55764 | 0.00030 | 0.00235 | 0.64184 | 0.00021 | 0.00250 |
| GCLM | 0.18137 | 0.48910 | 0.71718 | -1.24421 | 0.00000 | 0.00000 |
| GPx4 | 0.07350 | 0.62605 | 0.82867 | 0.56763 | 0.00676 | 0.04182 |
| GRX1 | 0.29823 | 0.20110 | 0.40651 | 2.16108 | 0.00009 | 0.00119 |
| ME1 | 0.37969 | 0.14378 | 0.32453 | 0.79444 | 0.00748 | 0.04514 |
| SOD1 | 0.03521 | 0.94323 | 1.00000 | -0.53206 | 0.00449 | 0.03027 |
| GCLC | -0.77948 | 0.00022 | 0.00181 | -0.55723 | 0.02518 | 0.11359 |
| GRX5 | -1.17113 | 0.00000 | 0.00000 | 0.41264 | 0.02221 | 0.10353 |
| GSS | 0.52491 | 0.01112 | 0.04694 | 0.12923 | 0.69909 | 0.90211 |
| MTHFD2 | -1.76775 | 0.00000 | 0.00000 | -0.32393 | 0.04243 | 0.16438 |
| PRDX1 | 0.70918 | 0.00001 | 0.00007 | -0.00554 | 1.00000 | 1.00000 |
| PRDX4 | -0.76080 | 0.00004 | 0.00039 | -0.31095 | 0.14998 | 0.38087 |
| GR | 0.20379 | 0.31774 | 0.55050 | -0.07234 | 0.70778 | 0.90693 |
| 6PGD | 0.40346 | 0.02157 | 0.07888 | -0.48224 | 0.01065 | 0.05932 |
| CAT | 0.43410 | 0.12796 | 0.29958 | -0.06134 | 0.91541 | 1.00000 |
| G6PD | 0.53432 | 0.03641 | 0.11827 | 0.42565 | 0.07038 | 0.22997 |
| GPx1 | -0.11793 | 0.63938 | 0.83796 | 0.20981 | 0.49977 | 0.76698 |
| GPx2 | -1.09321 | 0.63351 | 0.83478 | not expressed | | |
| GPx5 | not expressed | | | not expressed | | |
| GPx6 | not expressed | | | not expressed | | |
| GPx7 | 0.85049 | 0.35606 | 0.59151 | not expressed | | |
| GRX2 | 0.48896 | 0.16192 | 0.35076 | 0.09539 | 0.74649 | 0.93214 |
| GRX4 | not expressed | | | not expressed | | |
| GST | 0.21470 | 0.99888 | 1.00000 | -0.15027 | 0.75125 | 0.93478 |
| IDH2 | -0.67838 | 0.01454 | 0.05802 | 0.22542 | 0.37173 | 0.65304 |
| MTHFD1 | 0.26363 | 0.13023 | 0.30274 | 0.14841 | 0.44003 | 0.71723 |
| NNT | 0.29714 | 0.21809 | 0.42893 | -0.23764 | 0.81422 | 0.98562 |
| PRDX2 | 0.12871 | 0.43486 | 0.66898 | -0.01078 | 0.91246 | 1.00000 |
| PRDX3 | 0.09033 | 0.63888 | 0.83761 | -0.09467 | 0.73893 | 0.92743 |
| PRDX5 | 0.19037 | 0.32529 | 0.55776 | -0.28408 | 0.25664 | 0.53159 |
| PRDX6 | 0.29760 | 0.09558 | 0.24295 | 0.19599 | 0.27485 | 0.55494 |
| SOD3 | not expressed | | | not expressed | | |
| TXN1 | 0.13121 | 0.39574 | 0.63202 | -0.14490 | 0.39908 | 0.67966 |
| TXN2 | -0.31790 | 0.31745 | 0.55006 | -0.47557 | 0.45790 | 0.73389 |
| TXNRD1 | 0.14478 | 0.32651 | 0.55926 | -0.26647 | 0.04211 | 0.16362 |
| TXNRD2 | 1.31332 | 0.01732 | 0.06679 | 0.24360 | 0.51546 | 0.77717 |
| TXNRD3 | 0.35552 | 0.54112 | 0.76008 | -0.09352 | 0.85046 | 0.98524 |

ELAVL1(HuR) is included as a reference gene since it is the target of CRISPR/Cas9 editing and **It is the only non-anti-oxidant gene in this table.**

Significant Fold Change:
FDR <=0.05
log2 fold change +/- 0.58
pvalue <=0.05

Supplemental Methods

Detailed Mouse studies

Treatment groups for mouse experiments are detailed in the text, and included various dietary modifications, and/or gemcitabine treatment. For gemcitabine administration, the drug was suspended in normal saline at 5mg/mL and administered i.p. to mice at 100 mg/kg; vehicle was prepared at a volume of 20 μ l/g of 0.9%NaCl. For relevant experiments, drug was injected biweekly into the peritoneal cavity once the tumor diameter reached 50 mm³.

Mouse diets were modified to alter peripheral glucose levels and simulate nutrient withdrawal experiments performed *in vitro*, and nutrient withdrawal present in the PDA tumor microenvironment in patients. Prior mouse xenograft studies demonstrate that differences in peripheral glucose levels *in vivo* translate into even greater discrepancies within the mouse tumor microenvironment (15,16). Mice were therefore fed normal chow (NC) until tumors reached 50 mm³, and assigned one of the following diets: high carbohydrate diet (HC), ketogenic and calorie restricted diet at 75% of their average daily calorie intake (KCR75), and a ketogenic and calorie restricted diet at 50% of their caloric intake (KCR50). Specific dietary formulas were as follows: 1) HC (Bio-serve; F3155), carbohydrate 68%, protein 12.6%, fat 4.1%, 3.5 kcal/gm; 2) KCR (Bio-serve; F3666), carbohydrate 3.2%, protein 8.6%, fat 75.1%, 7.24 kcal/gm. Mice involved in calorie restricted experiments were singly caged for optimal dietary control, with no ill effects observed from this intervention. For *in vivo* experiments involving doxycycline (DOX) inducible gene suppression, the antibiotic was integrated into the chow formula at 200 mg/kg (HC+DOX; Bio-serve; F6987)(KC+DOX; Bio-serve; F7106). Serum glucose levels were tracked once per week using the AlphaTrak glucometer system (Abbott). Upon termination of mouse experiments, mice were euthanized using carbon dioxide inhalation followed by cervical dislocation, and

tumors harvested.

Bioenergetics analysis

Cells were seeded at 20,000 cells per well within 24 well Seahorse cell culture plates and allowed to grow for 24 hours. Using the Seahorse XF24 Extracellular Flux Analyzer, baseline measurements of the O₂ consumption rate (OCR) were recorded followed by leak dependent OCR (after addition of 500ng/mL oligomycin), maximal OCR (after addition of 100nM FCCP), and non-mitochondrial OCR (Antimycin 1uM). Measurements were normalized to total cellular protein/well using the BCA protein assay (Thermo Fisher Scientific).

Evaluation of IDH1 mRNA in pancreas clinical specimens

Previously reported microarray expression (21) data was downloaded from GEO (accession number: GSE71729). The dataset contains 46 normal pancreatic tissue samples, 145 primary pancreatic adenocarcinomas, and 61 metastatic pancreatic adenocarcinomas. Paired t-tests were performed to compare the differences between the three conditions. P values < 0.05 were considered statistically significant.

Immunohistochemistry (IHC)

Each sample was re-reviewed by an experienced surgical pathologist (W.J.) to confirm the histological diagnosis of PDA. TMAs were cut to 4µm thick sections and assayed with antibodies against HuR (Santa Cruz Biotechnologies; 5261 clone 3A2, 1:400) and IDH1 (Abcam; ab 184615, 1:100). All immunolabeled samples were given a total IHC score by a surgical pathologist, equivalent to the labeling intensity score (1, negative staining; 2, weak staining; 3, moderate staining; or 4, strong staining) multiplied by a score reflecting the percentage of labeled cells (0-10%=1, 10-50%=2, 50%-80%=3, >80%=4)(15). HuR staining was evaluated separately for cytoplasmic and nuclear staining. A total cellular HuR score was also

calculated, and equaled the sum of cytoplasmic and nuclear HuR scores. IHC scores were categorized for each protein, into tiered groups to facilitate statistical analyses. IDH1 scores were grouped as high (IHC score > 6), moderate (IHC score = 6) or low (IHC score < 6). HuR scores above 6 and 8 were categorized as high scores for cytoplasmic and total HuR scores, respectively; remaining samples were categorized as low. Associations between IDH1 and HuR IHC scores were determined using a χ^2 test. P values < 0.05 were considered as statistically significant.

RNA sequencing

RNA seq was performed on MiaPaCa2 and HS-766T modulated genetically by CRISPR/Cas9 to knockout HuR, along with the appropriate isogenic control cells. Cells were plated in 100mm³ dishes in triplicate, and incubated in 5mM glucose media for 24 hours (low glucose culture conditions). Total RNA was extracted using the RNeasy mini kit (Qiagen). The RNA was then deep sequenced on an Illumina NextSeq 500 machine. Sequence libraries were constructed following the manufacture's protocol; 2x75 bp paired-end reads and ~80 million reads were generated for each sample, and quality trimming on raw reads was performed using Cutadapt prior to sequence mapping (<http://journal.embnet.org/index.php/embnetjournal/article/view/200>). Sequence reads were aligned to the hg19 human genome build using the STAR aligning program (1). A two-pass alignment was performed and only those reads mapping uniquely to the human genome were maintained for further analysis. Quantification of all genes and their isoforms was performed using the RSEM algorithm, and the DESeq2 package was used to determine differentially expressed genes (2). Bioinformatics was performed for each of the two cell lines, comparing the expression levels of genes in the HuR (-/-) genes, compared to the isogenic control samples HuR

(+/-). P values and false-discovery rates (FDR) were calculated for each gene. Genes with gene expression changes that surpassed a log2 fold change +/- 0.58, FDR values ≤ 0.05 and p values ≤ 0.05 were identified as significantly changed from the control cell line to the HuR-knockout cell line. FPKM values for all genes in the coding transcriptome are provided, but the analysis for this study focused on 40 well characterized transcripts encoding enzymes directly involved in antioxidant defense. A heatmap including those genes that are significantly different in isogenic lines was generated using the ggplot2 program in R. Raw data are provided in Table S3.

Clinical outcome data

For the clinical correlation analysis, we analyzed records from 724 consecutive patients with PDA resected at Thomas Jefferson University Hospital between 2002 and 2014, after obtaining IRB approval. For the first analysis (Figure S2C and S2D), patients were grouped into 3 categories based on the Position Statement of the American Diabetes Association 2014 ($\text{HbA1C} \leq 6.5\%$, $6.5\% < \text{HbA1C} \leq 8.5\%$, $\text{HbA1C} > 8.5\%$). A total of 345 patients had available information. Parametric and non-parametric correlation studies were performed, along with ANOVA and post-hoc Bonferroni tests for HbA1C group comparisons. These tests were applied to determine the correlation of elevated HbA1C levels and pathologic features that are routinely reported on pathologic reports of resected specimens. Lymph node ratio (the number of regional lymph node metastases to total lymph nodes examined) was used as a surrogate marker of lymph node metastases.

In a separate survival analysis, disease free survival (DFS) data were available for a total of 107 patients who underwent pancreatic resection for localized disease at Thomas Jefferson University Hospital, and also received adjuvant gemcitabine (Table S2). An expanded definition of poor glycemic control was used, to optimize the sample size of the cohort with available data.

Patients were categorized into high glucose (HG, n=86) if they carried an existing diagnosis of diabetes or had a pre-operative HgbA1C > 6.0%. The remaining patients were categorized as having normal glucose (NG, n=21). Kaplan-Meier survival analysis and Cox multivariate hazard models were used for comparisons of survival. Adjusted covariates included tumor size, regional lymph node metastases, tumor grade, and glycemic status. P values < 0.05 were considered statistically significant. Statistical analysis was performed using the Statistical Package for Social Sciences (IBM SPSS, Ver.20, SPSS Inc., Chicago, IL, USA).

Supplemental Figure Legends

Figure S1, related to Figure 1: Low nutrient conditions promote PDA chemoresistance.

(A) Survival of PDA cell lines treated with the indicated doses of oxaliplatin. IC₅₀ values are provided. Cell survival was calculated by measurement of dsDNA content using PicoGreen. (B) Survival of PDA cells under the indicated conditions in the absence of chemotherapy by trypan blue staining. (C) ROS levels in MiaPaCa2 cells by DCF fluorescence under the indicated culture conditions for 24 hours. Gemcitabine (GEM 1 μ M) was administered at the time of nutrient withdrawal. Error bars represent \pm SEM of triplicate wells from a representative experiment. (* $p < 0.05$; ** $p < 0.01$; *** $p < 0.001$).

Figure S2, related to Figure 2: Low nutrient conditions induce PDA resistance to gemcitabine in mice and patients.

(A) Peripheral glucose levels were higher in mice fed a high carbohydrate (HC) diet, than mice fed a ketogenic and calorie restricted diet (75% of the average caloric intake, KCR75). Mice were treated with GEM as indicated. (B) Representative images of subcutaneous MiaPaca2 tumors, at the termination of the experiment (day 55). (C) Association of HbA1C levels and tumor size in resected PDA, with a corresponding correlation analysis (small panel). (D) Association of HbA1C levels and metastatic lymph node ratio in resected PDA, with a corresponding correlation analysis (small panel). (E) Schematic illustrating the effect of austere nutrient conditions on PDA cell growth and chemoresistance.

Figure S3, related to Figure 3: Dox-induced HuR silencing, along with a calorie restricted diet, suppresses PDA xenograft growth.

(A) Immunoblot of HuR protein expression of MiaPaCa2 cells modified with a doxycycline (DOX) inducible sh.HuR plasmid. Cells were

cultured in vitro and treated with 0 or 2 µg/ml of DOX for 5 days. (B) Peripheral glucose levels in mice fed a high carbohydrate (HC) diet, a ketogenic diet with 75% caloric intake (KCR75), or a ketogenic diet with 50% caloric intake (KCR50); mice were fed DOX as indicated. Each data point represents the mean ± SEM ($n=8$ per group). (C) Representative images of excised tumors of MiaPaCa2.sh.HuR and MiaPaCa2.sh.CTRL cells. Mice were fed an HC diet, KCR75 diet, or KCR50 diet. (D) qPCR-mRNA and immunoblot-protein validation of HuR suppression in MiaPaCa2.sh.HuR and MiaPaCa2.sh.CTRL cells. Each data point represents the mean ± SEM of three independent experiments * $p < 0.05$; ** $p < 0.01$; *** $p < 0.001$.

Figure S4, related to Figure 3: Low glutamine levels induce HuR nucleocytoplasmic shuttling. (A) Immunofluorescence demonstrates HuR subcellular localization to the cytoplasm (green cytoplasmic signal) when MiaPaCa2 cells are cultured in low glutamine media for 24 hours. GEM is used as a positive control that induces cytoplasmic HuR translocation (28). Magnification 40x. (B) Immunoblot of cytoplasmic MiaPaCa2 lysates incubated for 24 hours. GEM is used as a positive control. (C) PicoGreen cell survival assay at 5 days in MiaPaCa2 cells with declining levels of glutamine in the media. HuR overexpression or silencing was performed, along with siRNA controls. Representative immunoblots are shown. (D) Trypan blue staining in MiaPaCa2 and Panc-1 cells after HuR silencing, with cells cultured in high and low glutamine conditions. (E) PicoGreen cell survival assay in MiaPacCa2 cells under the indicated conditions, with declining levels of GEM. Each data point represents the mean ± SEM of three independent experiments * $p < 0.05$; ** $p < 0.01$; *** $p < 0.001$.

Figure S5, related to Figure 4: HuR detoxifies reactive oxygen species (A) Baseline oxygen consumption rates (OCR) in MiaPaca2 cells cultured as indicated for 24 hours. (B) ATP production levels in MiaPaCa2 cells cultured for 24 hours under the indicated conditions. (C) Citrate fractions with the indicated amounts of ^{13}C . The M2 fraction reveals glucose-derived carbon. Preparations were derived from MiaPaca2 CRISPR HuR(+/+) or HuR(-/-) cells cultured in 5mM glucose for 24 hours in the presence of [1,2- $^{13}\text{C}_6$]glucose tracer. Each data point represents the mean \pm SEM of three independent experiments. * $p < 0.05$; ** $p < 0.01$; *** $p < 0.001$. (D) Schematic depicting HuR's general influence on ROS levels. Despite enhanced mitochondrial function (yielding increased ROS production), increased ROS clearance likely yields a net reduction of intracellular ROS.

Figure S6, related to Figure 5: HuR regulates IDH1 mRNA. (A) In top panel, MiaPaCa2 cells were cultured in 25mM and 5 mM glucose media for 24 hours, In bottom panel MiaPaCa2 cells after HuR silencing were cultured in 5 mM glucose media for 24 hours and the expression of transcripts encoding enzymes that generate NADPH was measured by RT-qPCR. (B) qPCR-mRNA expression of IDH1 in MiaPaCa2.sh.HUR xenografts after doxycycline treatment, related to Figures S3C and S3D. (C) HuR RNP-IP. Abundance of IDH1 mRNA bound to HuR. GLUT1 and DCK serve as negative and positive controls, respectively (10,22). MiaPaCa2 cells were cultured in low glutamine (0.5 mM) for 24 hours. (D) HuR and IDH1 mRNA levels in HS-766T CRISPR HuR(+/+) or HuR(-/-) cells; immunoblot of IDH1 and HuR protein in the same cells. (E) Transient overexpression of HuR (or control empty vector) in Mia.HuR(-/-) and HS.HuR(-/-) cells (with CRISPR deletion of HuR), restored IDH1 expression in these cells, confirming HuR's importance for IDH1 expression. Each data point represents the mean \pm SEM of three

independent experiments. * $p < 0.05$; ** $p < 0.01$; *** $p < 0.001$.

Figure S7, related to Figure 5: IDH1 3'UTR deletion constructs confirmed HuR binding to the IDH1 transcript. (A) Schematic highlighting computationally predicted HuR binding sites in the 3'UTR of the IDH1 mRNA transcript. (B) MiaPaCa2 cells were co-transfected with an overexpression plasmid (HuR or empty vector) and luciferase reporter constructs (luciferase control or luciferase fused with IDH1 3' UTR). Cells were cultured in 5mM glucose media for 24 hours. (C) IDH1 3'UTR deletion series localizing the HuR binding region to the upstream 192bp of the IDH1 3'UTR, containing three predicted binding sites. Luciferase activity was tested after HuR overexpression. (D) MiaPaCa2 cells were cultured in 5mM glucose for 24 hours and IDH1 mRNA was measured after treatment with a transcription inhibitor (actinomycin D). IDH1 transcript levels were normalized to 18S. (E) α KG/citrate ratios measured by GC/MS, in Mia.HuR(-/-) or Mia.HuR(+/-) cells cultured under the indicated conditions for 24hours. Each data point represents the mean \pm SEM of three independent experiments. * $p < 0.05$; ** $p < 0.01$; *** $p < 0.001$.

Figure S8, related to Figure 6 and Figure 7: IDH1 expression protects PDA cells under stress, and rescues HuR-deficient PDA cells under stress. (A) IDH1 silencing. ROS levels in MiaPaCa2.si.IDH1 cells, as measured by DCF fluorescence. Cells were cultured under the indicated conditions for 48 hours, and GEM (1 μ M) for the last 18 hours, as indicated. (B) IDH1 overexpression. ROS levels in MiaPaCa2.IDH1OE cells, as measured by DCF fluorescence. Culture conditions were the similar to Figure S8B. (C) IDH1 overexpression. NADP⁺/NADPH ratio in Panc-1.IDH1OE and MiaPaCa2.IDH1OE cells cultured in 5 mM glucose media for 24

hours. (D) PicoGreen cell survival and drug sensitivity assays in MiaPaCa2 cells treated with GEM. (E) γ -H2AX foci. MiaPaCa2 cells were cultured in 5mM and 25mM glucose for 48 hours, and either GEM (1 μ M) or vehicle for the last 18 hours, as indicated. Each data point represents the mean \pm SEM of three independent experiments. (F) PicoGreen cell survival and drug sensitivity assays in MiaPaCa2 cells with IDH1 or HuR silencing. Cells were cultured in 5 mM glucose and treated with n-acetyl cysteine (NAC)(0.5mM/ml). (G) PicoGreen cell survival and drug sensitivity assays in MiaPaCa2 cells treated with GEM. IDH1 overexpression (or empty vector) was performed in Mia.HuR(-/-) knockout cells or Mia.HuR(+/+). * $p < 0.05$; ** $p < 0.01$; *** $p < 0.001$.